Smartphone-based measurement of water surface tension by capillary wave analysis

Gusein Bedirkhanov, Lorenzo Trombini, Sobinson Sony

University of Rennes, Department of Science and Properties of Matter(SPM), Rennes, 35700, France

Abstract. In this study, we propose a new, easy-to-use method for measuring the surface tension of water. Conventional methods for determining the liquid surface tension typically involve complicated and expensive tools, such as optical goniometers and tensiometers. However, our team has developed a simple and cost-effective approach utilizing a smartphone and readily available items to analyze the surface tension through capillary wave analysis.

In our experiment, we generated capillary waves on the surface of water using a loudspeaker. The wave patterns were then captured using a smartphone camera and analyzed using a Python algorithm. This algorithm efficiently distinguishes between bright and dark fringes, and accurately determines the wavelength at various frequencies. By using the dispersion relation, which highlights the connection between the wave frequency and wavelength, we were able to calculate the surface tension coefficient.

The experimentally obtained surface tension value, validated through linear regression, was found to be $\gamma = 69.6 \pm 0.6$ mN/m. This result closely aligns with the surface tension of water at 20°C, which is 72.75 ± 0.36 mN/m, as reported in the International Tables of the Surface Tension of Water from the Journal of Physical and Chemical Reference Data. [1]. The main reason for deviations from reference values is supposed to be the presence of impurities that strongly affect the surface tension [2].

Keywords: Surface tension, Surface waves, Capillary waves

1. Introduction

Capillary waves are small ripples that occur at the interface of water and air. These waves move along the interface with small wavelengths, and their behaviour is primarily governed by surface tension. Surface tension can be treated as an isotropic force per unit length, γ, that lies in the surface and is unaffected by changes in the shape or size of the surface. For capillary waves, surface tension is the dominant restoring force that attempts to bring the water surface back to a state of flatness. This restoring force enables the ripple to propagate.

When waves propagate on a fluid surface, gravity (g) and surface tension (γ) act as the forces that restore the flat surface of the liquid. These forces control the dispersion relation of the wave, which relates its wavelength (λ) to the vibration frequency (f), following the equation [3]:

$$\gamma = \frac{(2\pi f)^2 - g\left(\frac{2\pi}{\lambda}\right)}{\left(\frac{2\pi}{\lambda}\right)^3}\rho, \tag{1}$$

where ρ is the density.

Capillary waves correspond to the approximation $\lambda \ll 2\pi\sqrt{\frac{\gamma}{\rho g}}$. In this case, the gravitational term can be neglected and the equation (1) takes a simpler form:

$$\gamma = \frac{\rho\lambda^3 f^2}{2\pi} \tag{2}$$

This relationship outlines a method for determining the surface tension of liquid by measuring the wavelength of capillary waves, initiated with sound waves of various frequencies.

Usually, the measurement of surface tension requires the use of a device known as a tensiometer. This device is both expensive and sophisticated, and its operation requires professional training. Advancements in science have made technology accessible to everyone. Modern smartphones are equipped with powerful capabilities for processing data and taking measurements, although the accuracy of such measurements may be inferior to that obtained from professional equipment. Nevertheless, they still provide satisfactory results. An experiment using a smartphone must meet the following three criteria:

(i) Easy reproducibility

(ii) Automatic and fast data processing

(iii) Adequacy of the results obtained

The primary objective of the study was to use and develop a method for measuring surface tension by capillary waves that satisfies all the criteria mentioned above. Such a method has the potential for various applications. For example, measuring surface tension at home could assist in the early detection of various medical issues, such as diabetic nephropathy. Regular measurement of urine surface tension in potential patients can help in the timely identification of kidney function loss, thereby allowing for effective treatment [4].

2. Experiment

2.1. Experimental Setup

The setup, as shown in the Figure 1, is composed of different components: a standard paper cup with a height of 9.2 ± 1 mm was used as the testing container. The liquid depth was set to 20 ± 1 mm, which was determined after a few preliminary trials. We

observed that at this height, the surface waves produced by the Bose Revolve SoundLink speaker placed at the base of the cup were clearly visible.

The speaker was positioned horizontally due to its shape. Since the vibrations originated from the side of the instrument rather than from the top or bottom, it was necessary to place it horizontally. To avoid movement of the paper cup under strong vibrations, we used a clamp to secure the cup during the measurement.

One of the two smartphones was positioned on top of the cup to capture images. The exposure settings were adjusted as necessary to ensure clear images. The second smartphone, equipped with a frequency generator app, was used to regulate the frequency of the vibration. This phone was connected to the speaker via Bluetooth, thereby transmitting the frequency output through the speaker beneath the cup. The induced frequency was verified using a frequency checker on Phyphox. [5]
The experimental data was recorded in a dark room to bring out the dark and bright fringes more vividly by using the phone flashlight.

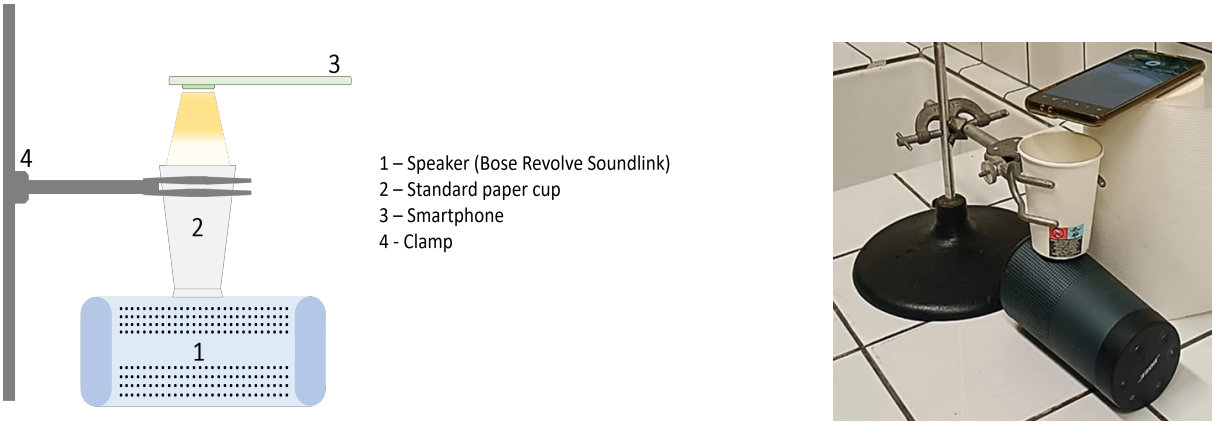

Figure 1: Experimental Setup

2.2. Experimental Procedure

To perform the experiment we decided to select a frequency range, which has been written in Table (1), with their associated wavelength values. The values of the frequency were visible on the phone paired with the speaker. The errors on these values were taken considering the discrepancy between the "frequency history" on Phyphox, which can capture the peak of the frequency on one phone, and the value set on the frequency generator app on the other phone. Thus obtaining, for each frequency used, a discrepancy of $\pm 1 Hz$‡.

Specific frequencies within this range were chosen after multiple trials, as the waves were observed to be visible in the photos and could be detected and processed efficiently by the algorithm. The selection of frequency was also dependent on the repeatability

‡ We neglected the frequency measurement error for calculating surface tension, since for our data they contribute to the measurement error 15 times less than the error from wavelength measurements

Table 1: Table of Corresponding Parameters: Frequency in Hertz, Wavelength in Pixels and Millimeters.

Frequency $[Hz]$	Wavelength $[pixel]$	Wavelength $[mm]$
104 ± 1	89.1 ± 0.5	0.344 ± 0.002
108 ± 1	87.7 ± 0.9	0.339 ± 0.003
110 ± 1	85.8 ± 0.7	0.331 ± 0.003
114 ± 1	82.6 ± 0.7	0.319 ± 0.003
116 ± 1	81.9 ± 1.2	0.316 ± 0.003
118 ± 1	83.2 ± 1.2	0.321 ± 0.005
121 ± 1	79.9 ± 1.2	0.308 ± 0.005
124 ± 1	77.7 ± 2.0	0.300 ± 0.008
127 ± 1	78.6 ± 1.3	0.304 ± 0.005

of achieving the surface waves consistently with a particular frequency, as it was seen to be extremely sensitive to the position of the cup, the surrounding environment, and other external factors.

For each frequency, around 15-20 photos were taken. The photos were taken by placing the phone as much as possible perpendicular to the water surface in order to avoid parallax. Moreover, the same divergence of flashlight, contrast with the surroundings, and focus were kept as much as possible. The measurement was repeated several times with the lowest possible alterations or disturbances to the initial system to obtain concurrent values.

While illuminating the capillary waves with light, each wave works as a lens, concentrating the light onto a small area at the bottom of the cup. Consequently, the image at the bottom of the cup reinstates the wave pattern with an equivalent wavelength, as illustrated in the Figure (2)

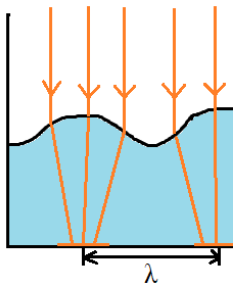

Figure 2: Capillary waves refract light

In Figure (3) some of the photos are presented, which were captured with the objective of ensuring that the data could be accurately calculated by the Python algorithm, which was able to differentiate between the color pixels. Even when the fringes were hardly noticeable in some of the photos to the naked eye, the wavelength could still be detected and calculated by the algorithm. Any photos that were of extremely poor quality were discarded and new ones were taken. With these photos, it was possible to proceed with data treatment and thus estimate the surface tension of water.

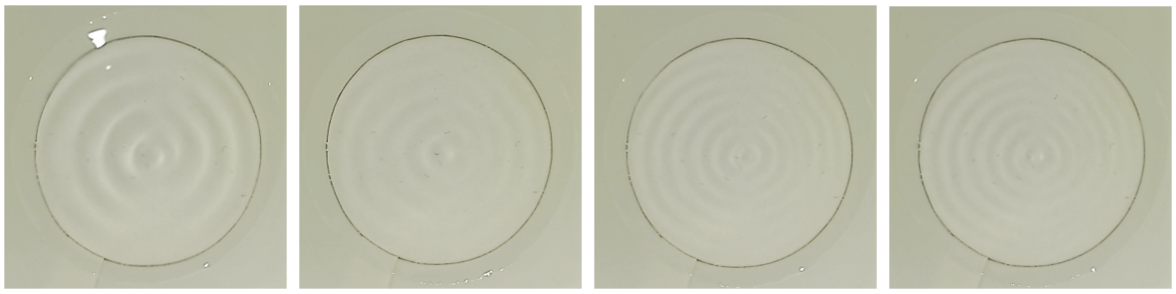

(a) (b) (c) (d)

Figure 3: Types of surface waves with different frequencies, captured by the camera of the smartphone. a) $104Hz$. b) $114Hz$. c) $124Hz$. d) $127Hz$

2.3. Data Treatment

Here we outline the steps for analyzing images obtained from the experiment. The treatment process involved multiple steps which are summarized below:

(i) The pictures taken by the phone were analyzed using Python code to define the borders of the cup. This helped to isolate the circle with the waves at the bottom, using Hough transform.

(ii) As can be seen from Figure (3), the waves are not visible with the same sharpness in different directions. Moreover, due to the rolling shutter effect (see Section (3.0.1)) we can't analyse picture in vertical direction. Therefore, a zoomed-in image of the left or right part of the picture was used to select an area where the fringes were more visible. This helped to condition the measurement and improve the accuracy of the results.

(iii) The code cut the picture following the selected area, Figure (4a), adjusted its contrast, and divided it into many horizontal lines to plot the profile of each line. This corresponded to the profile of the raw data, illustrated on the Figure (4b).

(iv) The profile was smoothed to find the maximum of the peaks, which were used as initial points for the approximation of the raw data with a Gaussian function. This function was centred based on the position of the points found before.

(v) The sequence of points was plotted to form a sequence of semi-circles that are concentric.

(vi) The position of these points was approximated using circles, as shown in Figure (4a, 4b). If the approximation did not converge using all the set of points, the code discarded the points at the borders, as the picture at the borders of the selected area in step 3 was not always enough contrast.

(vii) Using circles, it was possible to get two parameters: the position of the center with its coordinates $\{x_i, y_i\}$ and the radius $\{r_i\}$. The position of the circles was fixed considering the average of the $\{x_i, y_i\}$ to approximate a second of time and get the best radius value as possible.

(viii) The distance between each point and the circle to which they belong was calculated to discard 25% of the most distant points to the circle to which they belong.

(ix) Steps 6-7 were repeated once again to optimize the fit and obtain a set of radii $\{r_i\}$. The set of radii $\{r_i\}$ was analyzed, and the radii with more than $1.5 - pixel$ error were discarded.

(x) The set of wavelengths $\{\lambda_i\}$ was calculated as a distance between neighbouring radii.

(xi) All the wavelengths were analyzed based on two thresholds. The upper threshold was implemented since rarely the code was not able to distinguish wave surfaces with too low contrast, leading to anomalous values of the wavelengths. The second threshold was related to the effects of the borders, which led to the presence of too-close waves.

(xii) The set of wavelengths was measured in pixels, thus meaning that they needed to be converted in real distance, measured in mm. The conversion of λ_{pixel} to λ_{mm} used a scaling factor, the role of which is explained in the next section.

The mean values of the wavelengths coming from the bullet list have been used for the calculation of the surface tension (γ). The error of the mean value was calculated considering the distribution of the wavelengths, which followed the Gaussian distribution, and thus using the Equation (3), we were able to detect their errors ($\Delta\mu_i$).

$$\Delta\mu = t_{N-1}\frac{\sigma}{\sqrt{N}} \tag{3}$$

where $N \approx 60$ is the sample size, hence the number of wavelength used to calculate the mean value, σ is the experimental standard deviation, and the t_{N-1} — Student's coefficient.

Knowing the error on the pixel-based wavelength, we propagate it to find the respective discrepancy in the real-world distance. To propagate the error we used Equation (4).

$$\Delta\lambda_{mm} = |c|\Delta\lambda_{pixel} \tag{4}$$

where $|c| = 0.5/129.5$ is the absolute value of the scaling factor used.

2.4. Scaling factor for conversion of pixels to real-world distance

In order to determine the actual distance for the measured wavelength from the photos using the algorithm, we needed a scaling factor to convert the pixel distance in the photos to real-world distance. To achieve this, we positioned graph paper at the base of the cup, maintaining the same water level and keeping the rest of the setup unchanged. A photo of this setup was captured from the same height as the other photos, and it was analyzed to establish a relationship between unit distance and the number of pixels corresponding to that unit distance. We used the dimension of a square in the paper graph, measuring 0.5 cm, to calculate the distance in pixels using the software GIMP [6].

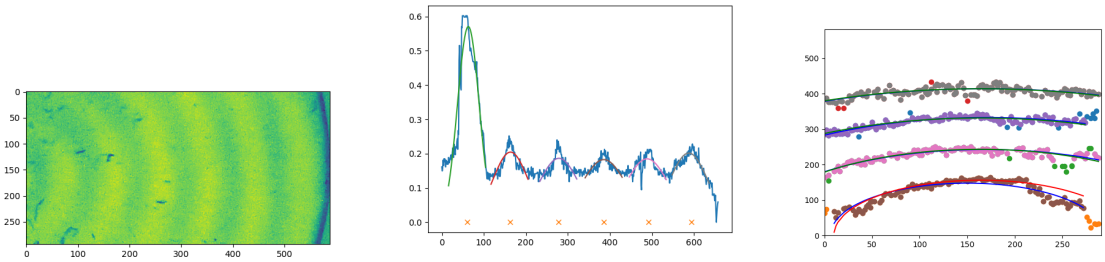

(a) (b) (c)

Figure 4: a) Cut of the picture made by the code, in which the yellow represents the bright fringes, and the green represents the dark fringes. The colour contrast is visible. b) Profile of a line along the horizontal direction for the image (a). Raw data are approximated with Gaussians. c) Approximation of the maxima using half circles. For each semicircle, a coloured representation of the points suitable for the approximation was chosen. Points of other colours are discarded by the code. Blue lines represent approximated circles without fixed positioning. Green lines are the final approximation with fixed centre position for circles. Bad approximations (red lines) were discarded

By drawing a line between two points, we obtained a relationship between pixel-based measurements and real-world distances. Positioning the paper graph in the cup parallel to the phone's camera, allowed us to work with two preferred directions (x-y directions) without needing to consider angles. To avoid errors due to the rolling shutter effect (see Section 3.0.1), we measured the wavelength in the horizontal direction, so the horizontal scaling factor was used.

3. Results and discussions

To calculate the surface tension, we used a linear regression of the λ^3 as a function of $\frac{2\pi}{f^2}$, as shown in Figure (5). The resulting fit would have had the surface tension (γ) as a slope, setting the intercept as zero. Thus, obtained value for the surface tension: $\gamma = (69.6 \pm 0.6)\frac{mN}{m}$.

In the introduction, we discussed the assumption that the gravitational term in Equation (1) is negligibly small. To illustrate this we plot the phase speed as a function of the wavelengths (dispersion law), given by the equation:

$$v = \sqrt{\frac{g\lambda}{2\pi} + 2\pi\frac{\gamma}{\lambda\rho}}. \tag{5}$$

If the gravitational term is neglected, the equation (5) becomes

$$v = \sqrt{2\pi\frac{\gamma}{\lambda\rho}}. \tag{6}$$

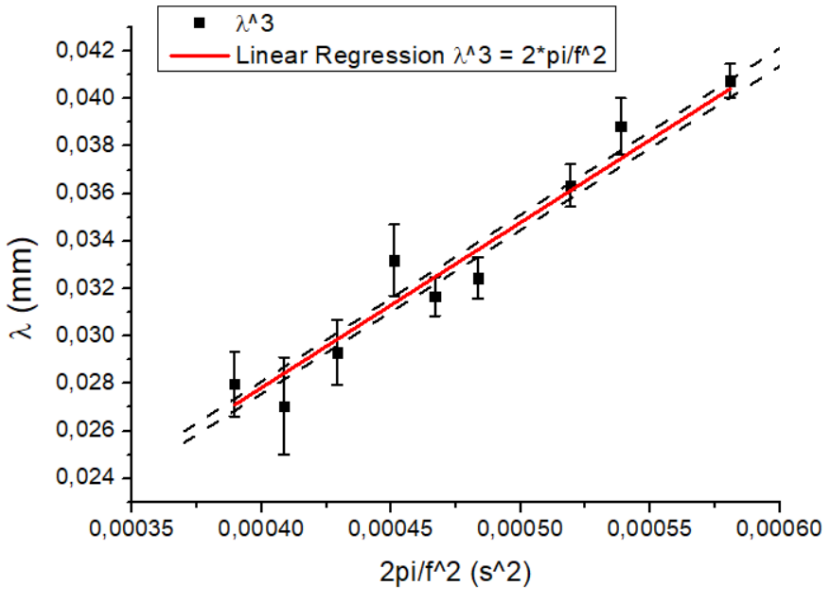

(a)

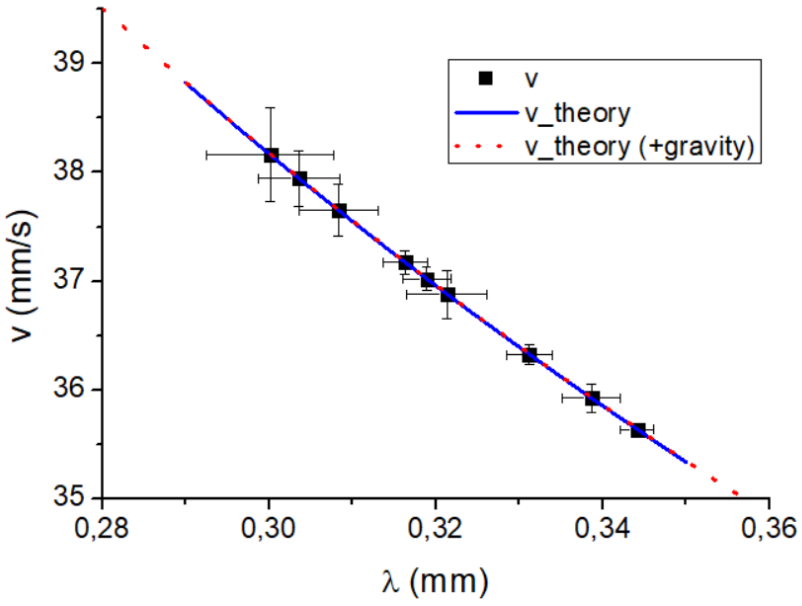

(b)

Figure 5: a) Dependence of λ^3 on $2\pi/f^2$ and the approximated line (red). The slope of the line equals the surface tension. The black lines represent are edge values of the surface tension following standard deviation b) Experimental and analytical (with and without the gravitational term) dispersion laws. As can be seen from the figure, the contribution from the gravitational term is negligible

The experimental and theoretical dispersion laws are illustrated in Figure (5.b). As we see, the gravitational term does not lead to any visible corrections to the experiment.

In the end of the section, we aim to discuss challenges encountered and some factors that could potentially introduce errors in the measurement and were tried to be taken into account.

3.0.1. Rolling-shutter effect Many smartphones have CMOS image sensor, which uses the so-called rolling-shutter mechanism [7] for taking pictures. While operating, CMOS image sensor activate rows of pixels one by one from up to bottom, and it can lead to image distortion. This results in a reduced observed wavelength for upward-propagating waves, and in contrast to an enlarged observed wavelength for downward-propagating waves compared to the real wavelength. To improve the accuracy of our wavelength measurements we considered wave propagation directions from left to right during data analysis.

3.0.2. Impact of temperature and impurities Another challenge was understanding how temperature and impurities affected the sensitivity of water surface tension. It was difficult to evaluate the level of impurities and their impact on surface tension compared to the reference value; even in the literature, the research of reference was extremely challenging, since giving a precise range of the level of impurities is tough. However, we found, in Figure (6b), that, based on our value of the surface tension, we expected a concentration of impurities around $0.1mM$. [2]. The temperature throughout the experiment has always been one of the most important parameters influencing measurement. In the literature, the surface tension value is extremely fluctuating, even using precise tools to evaluate it. Despite our efforts to maintain a constant temperature during measurements, we faced considerable difficulties in controlling it or making it vary less. [8]

3.0.3. Divergent beam of light The wavelength calculation assumed a parallel light beam originating from a flashlight on a phone, positioned approximately 14.5 cm above the cup bottom with a 2 cm radius. This corresponds to a divergence angle of 8 degrees (without taking into account the length of the light source). To validate the parallel beam assumption, reflections from water glare were observed (see Figure (7)).

If the beam divergence effect were significant, the reflections would appear much closer than the waves in the image at the bottom of the cap. However, the observed distances between highlights matched those between waves in the image at the bottom of the cap, supporting the validity of the initial assumption.

3.0.4. Border effect As the wave propagates from the cup centre to its edges, reflection occurs, resulting in interference and the formation of standing waves. The distance between standing wave antinodes deviates from the original wavelength. To mitigate the

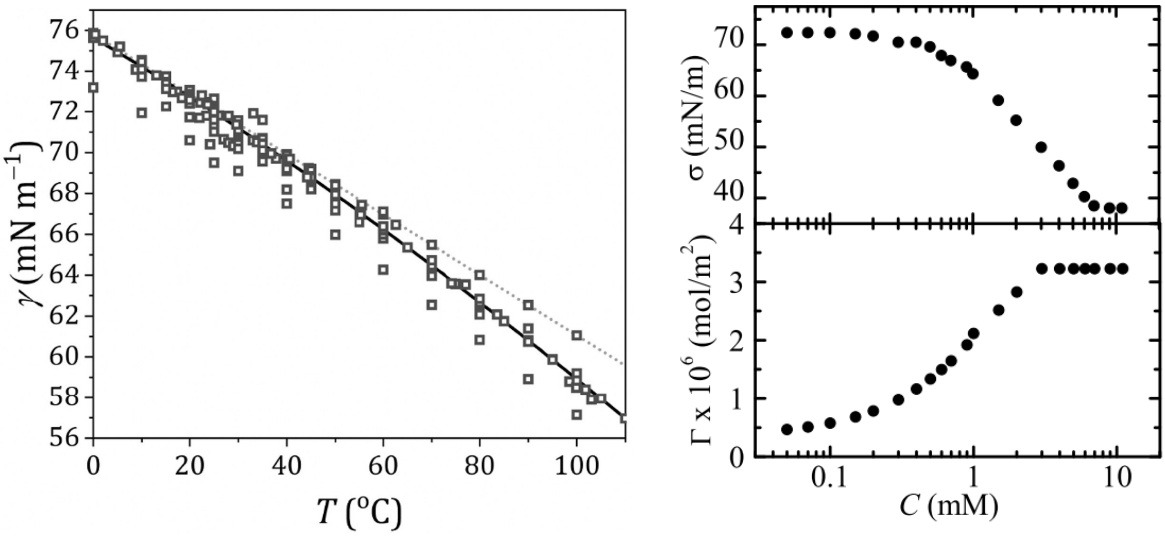

(a) (b)

Figure 6: a) Dependence of surface tension of water on the temperature.[8] b) Surface tension (σ) and surface density (Γ) for water as a function of the bulk surfactant concentration C. [2]

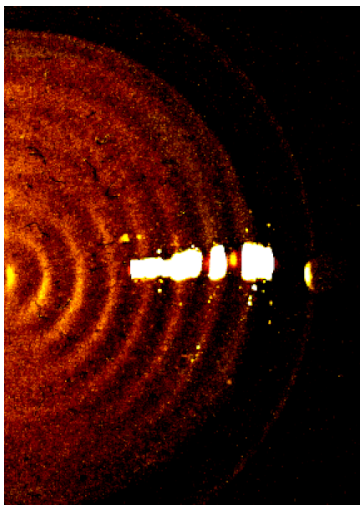

Figure 7: Contrast image of the reflected light with the wave picture at the bottom of the cap

impact of reflected waves, the speaker volume was reduced to minimize wave intensity at the cup boundaries, allowing for clear observation of a travelling wave.

4. Conclusions

In conclusion, we would like to note, that the proposed method used for measuring surface tension can hardly be used for practical measurements, at least with non-

professional equipment. A very strong dependence on the wavelength makes it difficult to apply simplifying assumptions and requires really precise measurements. We tried to overcome the last challenge by conducting multiple trials and using rigorous data validation processes to identify and minimize systematic or random errors. Additionally, employing a robust Python algorithm for data analysis helped enhance the accuracy and consistency of our measurements. This enables us to obtain an adequate value for the surface tension of water.

5. Acknowledgements

We want to express our deep appreciation to Professor Odin Christophe for allowing us to carry out a physics lab project using only our smartphones. Professor Christophe's support and encouragement were crucial in enabling us to explore innovative and unconventional approaches, creating a stimulating learning environment.

Additionally, we are sincerely grateful to our classmate, Maximillian Hanauske, for his generous contribution to our experiment. Max kindly lent us his speaker, an essential component used in generating the surface waves for our study. His collaborative spirit and willingness to share resources significantly enhanced the success of our project.

6. References

[1] Vargaftik, N.B., Volkov, B.N. and Voljak, L.D. (1983) 'International tables of the surface tension of water', Journal of Physical and Chemical Reference Data, 12(3), pp. 817–820.

[2] Ponce-Torres, A. and Vega, E. J., (2016) 'The effect of ambient impurities on the surface tension', EPJ Web of Conferences, 114, pp. 02098.

[3] Thorne, K.S. and Blandford, R.D. (2014) 'Chapter 16', in Modern classical physics: Optics, fluids, plasmas, elasticity, relativity, and statistical physics. Princeton: Princeton University Press.

[4] Donnan, W. D., Donnan, F. G. (1905). The Surface Tension Of Urine In Health And Disease: With Special Reference To Icterus. The British Medical Journal, 2(2347), 1636–1641

[5] Phyphox - physical phone experiments. Available at: https://phyphox.org/.

[6] 'GIMP ' (2023). The GIMP Development Team. Available at: https://www.gimp.org.

[7] Liu, Y. (2016). Decoding mobile phone image sensor rolling shutter effect for visible light communications. Optical Engineering, 55(1), 016103-016103.

[8] Oosterlaken, Bernette M. and de With, Gijsbertus (2022) 'How Reliable Are Surface Tension data?', Accounts of Materials Research, 3(9), pp.894-899.